БЪЛГАРСКА АКАДЕМИЯ НА НАУКИТЕ BULGARIAN ACADEMY OF SCIENCES
ТЕОРЕТИЧНА И ПРИЛОЖНА МЕХАНИКА THEORETICAL AND APPLIED MECHANICS
София, 1989, год. XX, № 1 Sofia, 1989, Year XX, No 1

Механика на твърдото деформируемо тяло

A family of finite elements for the analysis of box bridge decks

L. Boswell

1. Introduction

Continuous bridge decks may be analysed as three-dimensional structures using shell or plate elements. In cases of preliminary analysis or where other circumstances permit, however, a full three-dimensional analysis may not be necessary. There are obvious computational advantages to be gained if a three-dimensional structure can be represented adequately by a one-dimensional element idealisation. Although several researchers have extended beam elements for this purpose, they have considered only open section beams or single-cell boxes 1-4, 6-8, 11, 17.

The family of elements presented in this paper and in particular the general thin-walled box beam element, is capable of reducing the analysis of a bridge deck to a one-dimensional subdivision, whilst retaining the main structural actions. The available elements which are included in the family can be described as follows:

i) Two-node truss element,
i) Inclined cable element with catenary action,
iii) Two-node solid beam element,
iv) Three-node solid beam element,
v) Thin-walled box beam element with rigid cross-section,
vi) Thin-walled box beam element with deformable cross-section.

The thin-walled box beam element with deformable cross-sections may be regarded as the general element of the family and will, therefore, be considered in some detail. In addition to the usual six degrees of freedom at each node represented by the three translations and the three rotations, three more degrees of freedom have been incorporated in the formulation, to account for warping and distortion effects. These additional degrees of freedom are designated as the rate of change of twisting angle, the distortional angle of the cross-section and the rate of change distortional angle.

2. Formulation of the thin-walled box beam element
2.1. The definition of the element geometry

Consider the thin-walled box beam element with variable cross-sections shown in Fig. 1. The element is curved in space but the cross sections are generated by straight lines. A cross-section is assumed to have a vertical axis of symmetry to simplify the analysis of distortion, however, the requirement is unnecessary for the other elements in the family.

The element axis is defined as the locus of the centroids which may be distinct but parallel to the flexural axis (locus of the shear centres). The element has two end nodes and a midpoint node situated on the axis.

Two coordinate schemes are used in the element formulation: the Cartesian orthogonal coordinate system and the natural curvilinear coordinate system. The origin

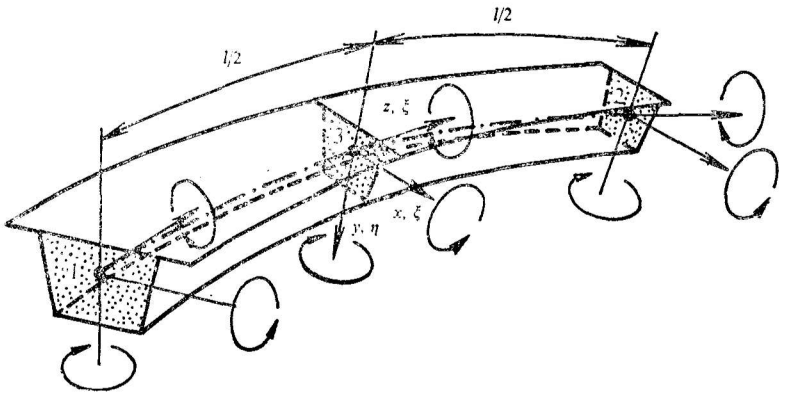

Fig. 1 Thin-walled box beam element with three nodes

of the Cartesian coordinate system is located at the centroid of the cross-section and the orientation of the local axes xy is assumed to coincide with the principal axes of the cross-section. The local z axis is tangential to the element axis in the direction of node 1 to node 2. The local y axis usually represents the vertical axis of symmetry; the local x axis being defined by a right handed orthogonal system. The origin of the natural coordinate system lies at the middle point of the element axis. It is assumed that ζ varies between -1 and $+1$ on the respective faces of the element. The geometry of the element axis is then defined as a mapped image of a parent straight element.

2.2. The displacement field

Using the theories of bending, warping torsion and distortion, the displacement field within an element

$$[u_x v_y w_z]^T \text{ or } [u_t v_n w_z]^T$$

can be related to the displacement components of the element [14,15]. For bending the displacements are

$$(1) \qquad u_b = \begin{Bmatrix} u_x \\ v_y \\ w_z \end{Bmatrix} = \begin{bmatrix} 1 & 0 & 0 & 0 & 0 \\ 0 & 1 & 0 & 0 & 0 \\ 0 & 0 & 1 & y & -x \end{bmatrix} \begin{Bmatrix} u \\ v \\ w \\ \theta_x \\ \theta_y \end{Bmatrix}$$

and for warping torsion and distortion the corresponding displacements are

$$(2)\qquad u_t=\begin{Bmatrix} u_t \\ v_n \\ w_z \end{Bmatrix}=\begin{bmatrix} R_t & 0 & V_s & 0 \\ 0 & 0 & V_n & 0 \\ 0 & -\widehat{\omega}_I & 0 & -\omega_{II} \end{bmatrix}\begin{Bmatrix} \theta_z \\ \theta_z' \\ \gamma_d \\ \gamma_d' \end{Bmatrix},$$

where u, v and w are the translations along the local xyz axes respectively, θ_x and θ_y are average rotations about the x and y axes respectively, which are given by

$$(3)\qquad \begin{Bmatrix} \theta_x \\ \theta_y \end{Bmatrix}=\begin{Bmatrix} \frac{\delta w}{\delta y}+\Phi_x \\ -\frac{\delta w}{\delta x}+\Phi_y \end{Bmatrix},$$

in which Φ_x and Φ_y denote the average shear deformation,[5]

θ_z is the angle of twist, θ_z' is the rate of distortion,

γ_d is the distortional angle, γ_d' is the rate of distortion,

R_t is the perpendicular distance from the shear centre to the tangent to the mid-line of the wall,

V_s is the distribution function of the tangential displacement in distortion.

V_n is the distribution function of the normal displacement in distortion,

$\widehat{\omega}_I$ is the unit torsional warping function, and

ω_{II} is the unit distortional warping function.

Thus the generalised displacements in the local coordinate system are given by

$$(4)\qquad \bar{u}=[u\ v\ w\ \theta_x\ \theta_y\ \theta_z\ \nu\ \gamma_d\ \psi_d]^T,$$

where $\nu=\frac{\delta\theta_z}{\delta z}$ and $\psi_d=\frac{\delta\gamma_d}{\delta z}$. The corresponding displacements in the global system are given by

$$(5)\qquad \delta=[U\ V\ W\ \theta_x\ \theta_y\ \theta_z\ \nu\ \gamma_d\ \psi_d]^T,$$

where U, V and W are the translations along the X, Y and Z global axes respectively, and Φ_x, Φ_y and Φ_z are the rotations about the same axes, respectively. The thin-walled box beam element has, therefore, nine degrees of freedom at each node. The other elements in the family may be suitably defined by decreasing the appropriate degrees of freedom, which become unnecessary for the description of their displacements.

2.3. Strain and stress resultants

The axial and shear strains for the element due to bending may be defined by

$$(6)\qquad \varepsilon_b=\begin{bmatrix} 1 & 0 & 0 & 0 & 0 \\ 0 & 1 & 0 & 0 & 0 \\ 0 & 0 & 1 & y & x \end{bmatrix}\bar{\varepsilon}_b,$$

where the generalised strain vector is

$$(7)\qquad \bar{\varepsilon}_b=\left[-\theta_y+\frac{\delta u}{\delta z}\ \theta_x+\frac{\delta v}{\delta z}\ \frac{\delta w}{\delta z}\ \frac{\delta\theta_x}{\delta z}\ \frac{\delta\theta_y}{\delta z}\right]^T.$$

The corresponding direct and shear stresses at a point within the element are given by

(8) $$[\sigma_z, {}_b\tau^b_{xz}\ \tau^b_{yz}]^T = D_b \varepsilon_b,$$

in which the elasticity matrix is

(9) $$D_b = \begin{bmatrix} E_1 & 0 & 0 \\ 0 & G & 0 \\ 0 & 0 & G \end{bmatrix},$$

where $E_1 = E/1-\nu^2$ and $G = E/2(1+\nu)$.

The strain energy due to warping torsion of the element may be defined by

(10) $$\varepsilon_t = \begin{bmatrix} \Phi_I & 0 \\ 0 & \widehat{\omega}_I \end{bmatrix} \widehat{\varepsilon}_{t'},$$

where the generalised strain vector is

(11) $$\bar{\varepsilon}_t = \left[\frac{\delta\theta_z}{\delta z} - \frac{\delta^2\theta_z}{\delta z^2}\right]^T.$$

The strain energy due to the secondary shear stresses associated with normal warping stresses is neglected for the present and only primary torsional shear strain will be considered. A warping shear parameter will be introduced later to account for the effects of secondary shear stresses. Thus, the function Φ_1 may be given by

(12) $$\Phi_1 = \left\{\frac{2y}{q_B t}\right\},$$

which is the sum of the St. Venant and Bredt contribution to the shear strain where

y_n is the normal coordinate to the midline of the wall,

q_B is the Bredt's unit shear flow function,

t is the thickness of the wall.

The corresponding stress components at a point within the element are given by

(13) $$[\sigma_z, {}_t\tau^t_{zs}]^T = D_t \varepsilon_t$$

in which the elasticity matrix is

(14) $$D_t = \begin{bmatrix} G & 0 \\ 0 & E_1 \end{bmatrix}.$$

The strain due to distortion of the element may be given by

(15) $$\varepsilon_d = \begin{bmatrix} \Phi_{II} & 0 \\ 0 & \omega_{II} \end{bmatrix} \bar{\varepsilon}_d,$$

where the generalised distortional strain vector is

(16) $$\bar{\varepsilon}_d = \left[\gamma_d - \frac{\delta^2\gamma_d}{\delta z^2}\right]^T$$

and the Φ_{II} function may be obtained from a transverse frame analysis. The distortional shear strain has been neglected.

The corresponding stress components are given by

(17) $$[\sigma_{db}\, \sigma_{z,d}]^T = D_d \varepsilon_d,$$

where the elasticity matrix is

(18) $$D_d = \begin{bmatrix} E_1 & 0 \\ 0 & E_1 \end{bmatrix}$$

and σ_{db} is the transverse distortional bending stress.

The substitution of all the above equations into the total potential energy expression and the subsequent integration enables the relation between the generalised stress resultants and the generalised strain components to be obtained as (Fig. 2)

$$\bar{\sigma}=\bar{D}\,\bar{\varepsilon}, \tag{19}$$

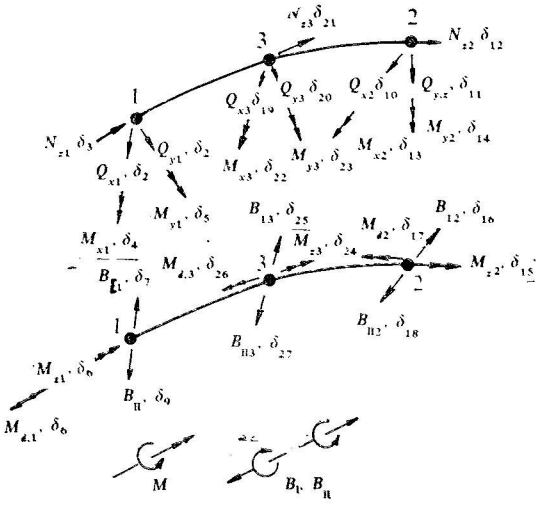

δ_i	Displ.	$\bar{\sigma}_i$	Force
$\delta_1\ \delta_{10}\ \delta_{19}$	u	$\bar{\sigma}_1\ \bar{\sigma}_{10}\ \bar{\sigma}_{19}$	Q_x
$\delta_2\ \delta_{11}\ \delta_{20}$	v	$\bar{\sigma}_2\ \bar{\sigma}_{11}\ \bar{\sigma}_{20}$	Q_y
$\delta_3\ \delta_{12}\ \delta_{21}$	w	$\bar{\sigma}_3\ \bar{\sigma}_{12}\ \bar{\sigma}_{21}$	N_z
$\delta_4\ \delta_{13}\ \delta_{22}$	θ_x	$\bar{\sigma}_4\ \bar{\sigma}_{13}\ \bar{\sigma}_{22}$	M_x
$\delta_5\ \delta_{14}\ \delta_{23}$	θ_y	$\bar{\sigma}_5\ \bar{\sigma}_{14}\ \bar{\sigma}_{23}$	M_y
$\delta_6\ \delta_{15}\ \delta_{24}$	θ_z	$\bar{\sigma}_6\ \bar{\sigma}_{15}\ \bar{\sigma}_{24}$	M_z
$\delta_7\ \delta_{16}\ \delta_{25}$	ν	$\bar{\sigma}_7\ \bar{\sigma}_{16}\ \bar{\sigma}_{25}$	B_I
$\delta_8\ \delta_{17}\ \delta_{26}$	γ_d	$\bar{\sigma}_8\ \bar{\sigma}_{17}\ \bar{\sigma}_{26}$	M_d
$\delta_9\ \delta_{18}\ \delta_{27}$	ψ_d	$\bar{\sigma}_9\ \bar{\sigma}_{18}\ \bar{\sigma}_{27}$	B_{II}

Fig. 2 Generalized forces and displacements
a) Distribution of the twisting angle along beam
b) Distribution of the distortional angle along the beam

where the generalised stress vector is

$$\bar{\sigma}=\left[Q_x\,Q_y\,N_z\,M_x\,M_y\,M_T\,\frac{1}{\mu_t}\,B_I\,M_d\,B_{II}\right]^T \tag{20}$$

and the generalised elasticity matrix is

$$\bar{D}=\begin{bmatrix} GA_{sx} & & & & & & & & \\ & GA_{sy} & & & & & & & \\ & & E_1A & & & & 0 & & \\ & & & E_1I_{xx} & & & & & \\ & & & & E_1I_{yy} & & & & \\ & & & & & GJ_T & & & \\ & & 0 & & & & \frac{1}{\mu_t}E_1J_1 & & \\ & & & & & & & E_1J_d & \\ & & & & & & & & E_1J_{II} \end{bmatrix} \tag{21}$$

where A_{sx} and A_{sy} represent the beam effective shear cross-sectional areas in the x and the y-directions respectively,
A is the cross-sectional area,
I_{xx}, I_{yy} are the moments of inertia with respect to the x and y axes respectively,
J_T is the total torsional moment of inertia,
J_I is the torsional warping moment of inertia,

μ_t is the warping shear parameter,
J_d is the distortional second moment of area, and
J_{II} is the distortional warping moment of inertia.
The generalised strain vector is

$$\bar{\varepsilon}=\left[-\theta_y+\frac{\delta u}{\delta z},\ \theta_x+\frac{\delta y}{\delta z},\ \frac{\delta w}{\delta z'}\ \frac{\delta\theta_x}{\delta z},\ -\frac{\delta\theta_y}{\delta z},\ \frac{\delta\theta_z}{\delta z},\ -\frac{\delta^2\theta_z}{\delta z^2},\ \gamma_d'-\frac{\delta^2\gamma_d}{\delta z^2}\right]. \tag{22}$$

In the above values the bending moments of inertia I_{xx} and I_{yy} have been calculated on the basis of an effective flange breadth replacing the actual width to account for the effect of 'shear lag'.[12]

2. 4. Shape functions for mapping element geometry

The normalised coordinates can be transferred to a curvilinear set when plotted in a Cartesian space by using an interpolation function with natural coordinate ζ. Thus, for each element

$$G=MG^e, \tag{23}$$

where G is the geometrical function of the element, G^e the corresponding nodal values and M is the geometrical shape function in terms of the natural coordinate. The form of transformation which has been used is referred to as hierarchical mapping. For a one-dimensional element the associated hierarchical shape functions are defined in terms of the natural coordinate ζ, that is

$$\begin{aligned} M_i&=\frac{1}{2}(1+\zeta_0) \quad \text{for } i=1 \text{ and } 2\\ M_i&=(1-\zeta^2) \quad \text{for } i=3, \end{aligned} \tag{24}$$

where

$$\zeta_0=\zeta.\zeta_i.$$

2.5. Shape functions for defining the displacement field

The displacement field $\bar{\delta}$, in the global coordinate system can be expressed in terms of a set of nodal displacements $\bar{\delta}^e$ by the use of suitable shape functions

$$\bar{\delta}=N\delta^{-e}. \tag{25}$$

Only C_0 continuity is required for the element axial and flexural effects and the corresponding shape functions become

$$\begin{aligned} N_i&=\frac{1}{2}(\zeta^2+\zeta_0) \quad \text{for } i=1 \text{ and } 2\\ N_i&=(1-\zeta^2) \quad \text{for } i=3 \end{aligned} \tag{26}$$

where

$$\zeta_0=\zeta.\zeta_1.$$

Since the potential energy functional due to warping torsion and distortion contains second derivatives and the governing differential equation of the problem is of fourth order, it is necessary to satisfy C_1 continuity for the element. The shape functions then become

$$\bar{N}_{11}=\frac{\zeta^2}{4}(4-5\zeta-2\zeta^2+3\zeta^3),$$

$$\bar{N}_{12}=\frac{J_1}{4}\zeta^2(1-\zeta)(1-\zeta^2),$$

(27)
$$\bar{N}_{21}=\frac{\zeta^2}{4}(4+5\zeta-2\zeta^2-3\zeta^3),$$

$$\bar{N}_{22}=\frac{J_2}{4}\zeta^2(1+\zeta)(\zeta^2-1),$$

$$\bar{N}_{31}=(1-\zeta^2)^2,$$

$$\bar{N}_{32}=J_3\zeta(1-\zeta^2)^2$$

for warping torsion and distortion generalised displacements, where J_1, J_2 and J_3 are the nodal Jacobian factors and are given by

(28)
$$J=\frac{\partial z}{\partial\zeta}=\sqrt{\left(\frac{\partial X}{\partial\zeta}\right)^2+\left(\frac{\partial Y}{\partial\zeta}\right)^2+\left(\frac{\partial Z}{\partial\zeta}\right)^2}.$$

Equations (27) are derived by considering a general interpolation function which is expressed as

(29)
$$f=\bar{N}_{11}f_1+\bar{N}_{12}\left(\frac{\partial f}{\partial z}\right)_1+\bar{N}_{21}f_2+\bar{N}_{22}\left(\frac{\partial f}{\partial z}\right)_2+\bar{N}_{31}f_3+\bar{N}_{32}\left(\frac{\partial f}{\partial z}\right)_3,$$

where f_i is the value of the unknown function at node i and $\left(\frac{\partial f}{\partial z}\right)_i$ is the first derivative which is

(30)
$$\frac{\partial f}{\partial z}=J^{-1}\left[\frac{\partial\bar{N}_{11}}{\partial\zeta}f_1+\frac{\partial\bar{N}_{12}}{\partial\zeta}\left(\frac{\partial f}{\partial z}\right)_1+\frac{\partial\bar{N}_{21}}{\partial\zeta}f_2+\frac{\partial\bar{N}_{22}}{\partial\zeta}\left(\frac{\partial f}{\partial z}\right)_2+\frac{\partial\bar{N}_{31}}{\partial\zeta}f_3+\frac{\partial\bar{N}_{32}}{\partial\zeta}\left(\frac{\partial f}{\partial z}\right)_3\right].$$

Since three discrete nodes are specified for each box beam element the shape function can be represented by a fifth order polynomial

(31)
$$\bar{N}=A_1+A_2\zeta+A_3\zeta^2+A_4\zeta^3+A_5\zeta^4+A_6\zeta^5.$$

Equations (27) are then obtained by noting that $\bar{N}_{i1}=1$ and $\frac{\partial N_{i2}}{\partial\zeta}=1$ at node i but is zero at all other nodes.

2.6. Formulation of displacements and strains

It is necessary to transform the local displacements to those relative to the global axes. This transformation is given by

(32)
$$\bar{u}=\lambda\bar{\delta}$$

in which λ is the transformation matrix.

By combining Equations (25) and (32) the generalised displacements in the local coordinate system are

(33)
$$u=\bar{N}\bar{\delta}^e=[\bar{N}_1\,\bar{N}_2\,\bar{N}_3]\bar{\delta}^e,$$

where $\bar{\delta}^e$ are the nodal values of the global displacements and

$$\bar{\bar{N}}_i =$$

$$\begin{bmatrix}
N_i\hat{i}\,\hat{x} & N_i\hat{j}\,\hat{x} & N_i\hat{k}\,\hat{x} & 0 & 0 & 0 & 0 & 0 & 0 \\
N_i\hat{i}\,\hat{y} & N_i\hat{j}\,\hat{y} & N_k\hat{k}\,\hat{y} & 0 & 0 & 0 & 0 & 0 & 0 \\
N_i\hat{i}\,\hat{z} & N_i\hat{j}\,\hat{z} & N_i\hat{k}\,\hat{z} & 0 & 0 & 0 & 0 & 0 & 0 \\
0 & 0 & 0 & N_i\hat{i}\,\hat{x} & N_i\hat{j}\,\hat{x} & N_i\hat{k}\,\hat{x} & 0 & 0 & 0 \\
0 & 0 & 0 & N_i\hat{i}\,\hat{y} & N_i\hat{j}\,\hat{y} & N_i\hat{k}\,\hat{y} & 0 & 0 & 0 \\
0 & 0 & 0 & \bar{N}_{i1}\hat{i}\,\hat{z} & \bar{N}_{i1}\hat{j}\,\hat{z} & \bar{N}_{i1}\hat{k}\,\hat{z} & \bar{N}_{i2} & 0 & 0 \\
0 & 0 & 0 & \dfrac{\partial N_{i1}\hat{i}\,\hat{z}}{\partial z} & \dfrac{\partial \bar{N}_{i1}\hat{j}\,\hat{z}}{\partial z} & \dfrac{\partial \bar{N}_{i1}\hat{k}\,\hat{z}}{\partial z} & \dfrac{\partial \bar{N}_{i2}}{\partial z} & 0 & 0 \\
0 & 0 & 0 & 0 & 0 & 0 & 0 & \bar{N}_{i1} & \bar{N}_{i2} \\
0 & 0 & 0 & 0 & 0 & 0 & 0 & \dfrac{\partial \bar{N}_{i1}}{\partial z} & \dfrac{\partial \bar{N}_{i2}}{\partial z}
\end{bmatrix} \tag{34}$$

where $\hat{i}.\hat{x}$, $\hat{j}.\hat{x}\ldots$, $\hat{k}.\hat{z}$ are the direction cosines.

With the displacements known within the element the strains are obtained from

$$\bar{\varepsilon} = L\bar{u}, \tag{35a}$$

where L is a linear operator given by

$$L =$$

$$\begin{bmatrix}
\dfrac{\partial}{\partial z} & 0 & 0 & 0 & -1 & 0 & 0 & 0 & 0 \\
0 & \dfrac{\partial}{\partial z} & 0 & 1 & 0 & 0 & 0 & 0 & 0 \\
0 & 0 & \dfrac{\partial}{\partial z} & 0 & 0 & 0 & 0 & 0 & 0 \\
0 & 0 & 0 & \dfrac{\partial}{\partial z} & 0 & 0 & 0 & 0 & 0 \\
0 & 0 & 0 & 0 & -\dfrac{\partial}{z} & 0 & 0 & 0 & 0 \\
0 & 0 & 0 & 0 & 0 & \dfrac{\partial}{\partial z} & 0 & 0 & 0 \\
0 & 0 & 0 & 0 & 0 & 0 & -\dfrac{\partial}{\partial z} & 0 & 0 \\
0 & 0 & 0 & 0 & 0 & 0 & 0 & 1 & 0 \\
0 & 0 & 0 & 0 & 0 & 0 & 0 & 0 & -\dfrac{\partial}{\partial z}
\end{bmatrix}$$

The strain matrix B is then obtained by combining equations (33) and (35 a), hence

$$\bar{B} = L\bar{\bar{N}} \tag{36}$$

$$\text{and} \quad \bar{\varepsilon} = \bar{B}\,\bar{\delta}^e. \tag{37}$$

2.7. The element stiffness matrix and equivalent nodal forces

The element stiffness matrix which is of the order 27×27 is expressed by the usual relationship

(38a) $$K^e = \int_{-l/2}^{+l/2} \bar{B}^T \bar{D}\, \bar{B} dz = \int_{-1}^{+1} J \bar{B}^T \bar{D}\, \bar{B} d\zeta.$$

Equation (38a) is integrated numerically by a Gauss quadrature and thus may be written

(38b) $$K^e = \sum_{i=1}^{n} H_i \left(\bar{B}^T \bar{D}\, \bar{B} \sqrt{\left(\frac{\partial X}{\partial \zeta}\right)^2 + \left(\frac{\partial Y}{\partial \zeta}\right)^2 + \left(\frac{\partial Z}{\partial \zeta}\right)^2} \right)_i,$$

where H_i is the weight coefficient and n is the number of sampling points. The exact integration of equation (38) may be achieved by using a three point quadrature for the axial and bending contributions and a six point quadrature for the torsional and distortional contributions. Since shear deformation has been included in the formulation for which the rotations due to bending are interpreted as shear strains, an excess of shear strain energy is stored by the element. This problem can be overcome by using a reduced integration scheme [16]. Thus, the two point integration procedure, which exactly integrates the bending contribution, but underintegrates the shear contribution, is used. The element performance is greatly improved and yields accurate results for both thick and thin beams.

The consistent force vector due to body forces is

(39) $$(F^e)^{B \cdot F} = \rho \sum_{i=1}^{n} H_i \left(\bar{N}^T b A \sqrt{\left(\frac{\partial X}{\partial \zeta}\right)^2 + \left(\frac{\partial Y}{\partial \zeta}\right)^2 + \left(\frac{\partial Z}{\partial \zeta}\right)^2} \right)_i,$$

in which ρ is the specific weight of the element material and A is the cross-sectional area. For bridge deck analysis it is usual to define the global Y axis to be normal to the level plane for which case the body force vector becomes

(40) $$b = [\hat{j}.\hat{x}\ \hat{j}.\hat{y}\ \hat{j}.\hat{z}\ 0\ 0\ \hat{j}.\hat{x}(Y_G - Y_S)\ 0\ -1/2\,\hat{j}.\hat{x}(Y_G - y_X)\ 0]^T,$$

where $\hat{j}.\hat{x}$, $\hat{j}.\hat{y}$, $\hat{j}.\hat{z}$ are the direction cosines of the Y axis relative to the local x, y and z axes respectively, y_G and y_S are the ordinates of the centroid and the shear centre measured from the mid-line of the top flange, respectively.

The consistent force vector due to distributed forces is written as

(41) $$\{F^e\}^{D \cdot F.} = \sum_{i=1}^{n} H_i \left(\bar{N}^T q^e \sqrt{\left(\frac{\partial X}{\partial \zeta}\right)^2 + \left(\frac{\partial Y}{\partial \zeta}\right)^2 + \left(\frac{\partial Z}{\partial \zeta}\right)^2} \right)_i,$$

in which the distributed force vector is

(42) $$q^e = [P_x\ P_y\ P_z\ m_{x,\,\mathrm{ext}}\ m_{y,\,\mathrm{ext}}\ m_{z,\,\mathrm{ext}} b_I m_d b_{II}]^T.$$

The distributed components per unit length are related to the local coordinate system and are assumed to be constant along the element.

The statically equivalent nodal forces due to the applied concentrated forces can be expressed as

(43) $$\{F^e\}^{P \cdot F.} = \Sigma N^T P.$$

The point of application of a concentrated load is defined by the natural coordinate ζ and the local coordinates x and y. The concentrated force vector is defined in global coordinate system as

(44) $$P = [\bar{P}_x\ \bar{P}_y\ \bar{P}_z\ \bar{M}_x\ \bar{M}_y\ \bar{M}_z\ 0\ \bar{M}_d\ 0\ ]^T$$

in which

$$\bar{P}_x = P_x(\hat{i}\,\hat{x})_\zeta + P_v(\hat{j}\,\hat{x})_\zeta + P_i(k\,x)_\zeta$$

$$\bar{P}_v = P_x(\hat{i}\,\hat{y})_\zeta + P_v(\hat{j}\,\hat{y})_\zeta + P_i(\hat{k}\,\hat{y})_\zeta$$

$$\bar{P}_z = P_x(\hat{i}\,\hat{z})_\zeta + P_v(\hat{j}\,\hat{z})_\zeta + P_i(\hat{k}\,\hat{z})_\zeta$$

$$\bar{M}_x = M_{x.\,\mathrm{ext}}(\hat{i}\,\hat{x})_\zeta + M_{v.\,\mathrm{ext}}(\hat{j}\,\hat{x})_\zeta + M_{z.\,\mathrm{ext}}(\hat{k}\,\hat{x})_\zeta + \bar{P}_i y$$

$$\bar{M}_y = M_{x.\,\mathrm{ext}}(\hat{i}\,\hat{y})_\zeta + M_{v.\,\mathrm{ext}}(\hat{j}\,\hat{y})_\zeta + M_{z.\,\mathrm{ext}}(\hat{k}\,\hat{y})_\zeta + \bar{P}_z y$$

$$\bar{M}_z = M_{x.\,\mathrm{ext}}(\hat{i}\,\hat{z})_\zeta + M_{v.\,\mathrm{ext}}(\hat{j}\,\hat{z})_\zeta + M_{z.\,\mathrm{ext}}(\hat{k}\,\hat{z})_\zeta + \bar{P}_y x - \bar{P}_x(y - y_S + y_G)$$

(45) $$\bar{M}_d = \frac{1}{2}\left[\left(\frac{b_b}{b_I}\,1\right)\bar{P}_y x + 2\bar{P}_x(y - y_S + y_G) + \bar{M}_i\right]\cdot|x| \leq \frac{h_i}{2}$$

and

$$\bar{M}_d = \frac{1}{2}\left[\left(\frac{b_b}{b_i} - 1\right)\bar{P}_v x - \left(1 + \frac{b_b}{b_i}\right)(1-\zeta_d)b_i + 2\bar{P}_k(y - y_S + y_G) + \bar{M}_i\right]\cdot|x| \geq \frac{b_i}{2},$$

where $b_x = x - b_t/2$ $(x>0)$, or $b_x = x + b_t/2$ $(x<0)$,

b_t and b_b are the widths of the top and bottom flanges between the side corner points respectively.

y_S and y_G are the vertical ordinates of the shear centre and the centroid with reference to the mid-line of the top flange, respectively,

and ζ_d is the distribution factor which can be obtained from the analysis of a frame formed from a unit slice of the box beam.

It should be noted that additional distortional forces occur in box beams curved in plan due to the radial component, σ_B, of the longitudinal bending stresses, $\sigma_{z,b}$. For unit length of the box,

(46) $$\sigma_R = \sigma_{z,b}/R,$$

where R is the radius of curvature which is positive when the centre of curvature is on the positive side of the x axis.

The system of radial forces can be replaced by a horizontal forces through the shear centre and a torsional moment. Thus, the additional distortional moment per unit length can be expressed as

(47) $$m_{d,R} = \mu_d M_x$$

in which μ_d is the initial curvature multiplication factor and is given by

(48) $$\mu_d = \frac{0.5}{I_{xx}} \int_A y\,[y - (y_S - y_G)]\,dA.$$

The implementation of the boundary condition is straightforward. The evaluation of the internal forces at the ends of the individual elements can be carried out following the standard finite element procedure, although in Ref. 15 a slightly modified procedure has been adopted.

3. Use of elements in bridge deck analysis

In order to use the elements which have been developed in the previous section special procedures should be adopted.

For single and multi-cell box beams, the longitudinal direction of the deck may be conveniently sub-divided into beam elements. In order to assess transverse effects, however, a transverse frame analysis must be undertaken for a unit length of cross-section[15].

For multi-spined box beams a grillage analogy is employed. It may be shown that due to distortion the top flange which connects adjacent spines rotates not only through the pure angle of twist, but additionally through half the distortional angle [9]. To account for this effect a reduced torsional stiffness is used but this may be calculated only after an initial deformation. Thus, an iterative procedure is used for this part of the analysis. The torsional stiffness reduction factor is given by

$$\zeta_d = \theta_z / \psi_z, \tag{49}$$

where

$$\psi_z = \theta_z + 1/2\gamma_d. \tag{50}$$

The grillage analogy is also used for the analysis of articulated bridge decks To account for the release of the bending moment across an articulation, a static condensation procedure is used which releases the moment.

In the case of cable-stayed bridges a Newton-Raphson procedure is used to account for the geometrically large displacement effect and the caternary action of the inclined cables.

4. Applications

4.1. Model tests

The appropriateness of the elements and the accuracy of the results obtained have been demonstrated by a theoretical and experimental comparison for the following models:

Model 1 — straight cantilever single cell box beam,
Model 2 — curved cantilever single cell box beam,
Model 3 — two-span continuous double cell box beam,
Model 4 — simply supported twin-box beam with trapezoidal cross-section.

The longitudinal distributions of the angles of twist and distortion for Model 1 are shown in Fig. 3. The close agreement between the theoretical and experimental values indicates that the additional degrees of freedom, which represent the warping and distortion can be included in the thin-walled box beam formulation to produce accurate results.

Typical examples of the comparison between the experimental stresses and those obtained both from the beam element and the LUSAS thin shell box element for the curved box model are given in Fig. 4 [10].

It is not possible to show all the theoretical and experimental comparisons. However, it may be stated that close agreement was found in all cases.

4.2. Practical bridge analysis

In order to demonstrate the application of the one-dimensional finite element family to practical bridge analysis, two actual bridge structures have been analysed. Figure 5 shows a simply supported prestressed concrete bridge[13]. The figure shows a comparison between the results obtained both from the thin-walled box beam element and the shell element of the LUSAS system.

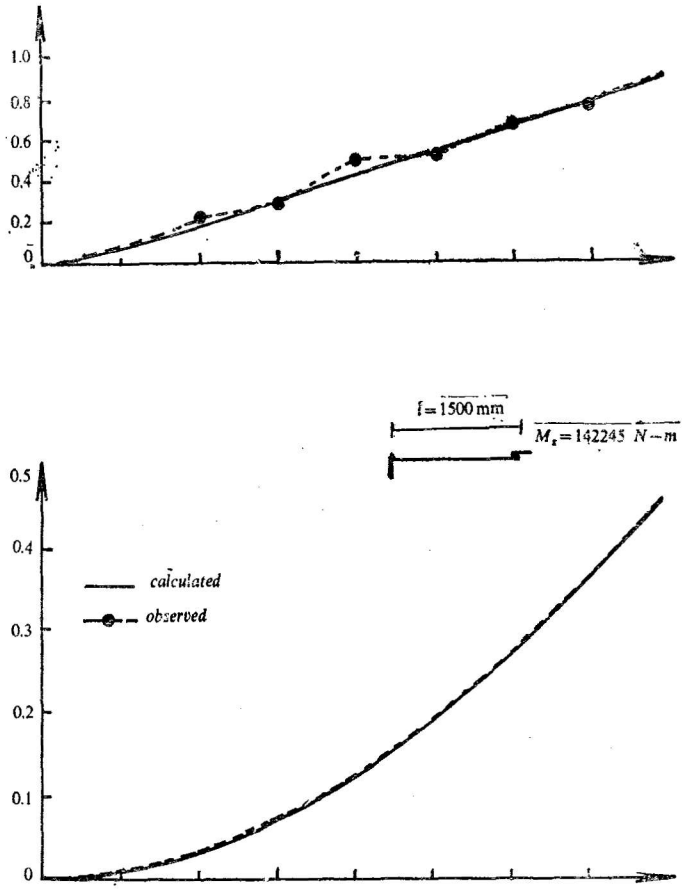

Fig. 3 Theoretical & experimental values in Model 1

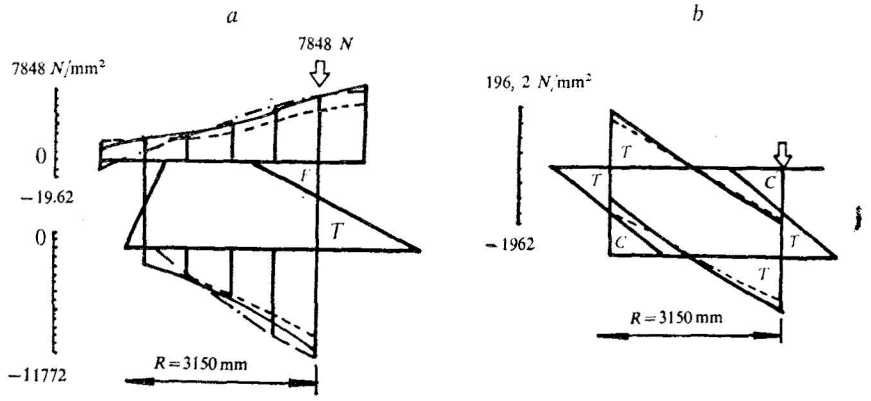

Fig. 4 Model 2:
a) Longitudinal membrane stresses
b) Transverse bending stresses at outer surface
— Present study
— Experimental results
— Thin shell box element solution

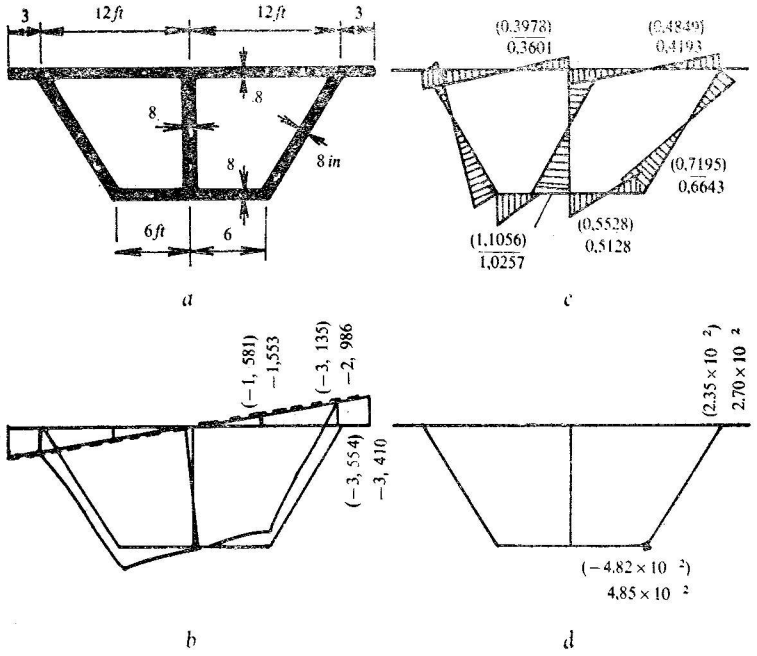

Fig. 5 A double-cell box beam
a) Cross-section and loading
b) Deflections at midspan (10 in)
c) Transverse bending moments at midspan (kip-in/in)
d) Warping stresses at midspan (kip/in)

Table 1

Comparison of measured and calculated values

Sections	Loading position	Measured values	Calculated values	Difference, as a percentage
(*a*) Axial forces of cables in kg (1 kg = 9.81 N)				
Cables				
Side-span 3′	(1)	23470	24945	+6.3
Side-span 4′	(1)	32990	37911	+14.9
Side-span 5′	(1)	57030	65414	+14.7
Mid-span 3′	(1)	27650	29979	+8.7
Mid-span 4′	(1)	36890	41960	+13.7
Mid-span 5′	(1)	55830	66285	+18.7
(*b*) Maximum stresses at bottom reinforcement, in kg/cm³				
Girder				
Sidespan	(2)	+197	+219	+11.2
Midspan	(1)	—289	—271	—6.2
(*c*) Deflection, in mm				
Girder				
Sidespan	(1)	1.90	2.340	+23.2
Midspan	(1)	12.85	14.938	+16.2
Tower ton	(1)	42.0	49.0	+16.7

The final example considers the Santal cable-stayed bridge, which spans the Pujiang River in China (Fig. 6). Table 1 compares some results obtained from actual field loading tests with those obtained from an analysis using the one-dimensional elements including non-linear effects.

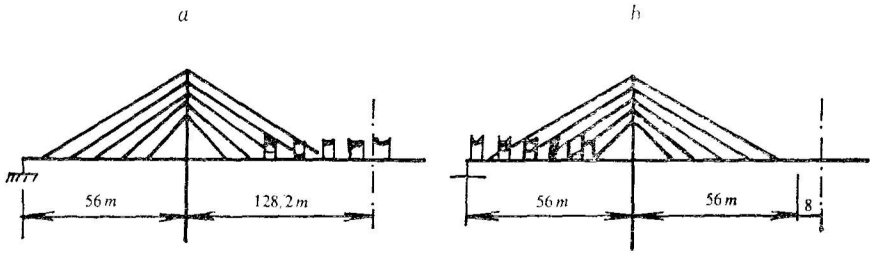

Fig. 6 Longitudinal positions of vehicle
a) Loading position 1
b) Loading position 2

5. Conclusion

A family of one-dimensional, sub-parametric elements, which are suitable for the elastic analysis of a variety of bridge decks, has been developed. In particular, the ability of one-dimensional elements to analyse box-type bridge decks has been extended.

The performance of the elements has been compared favourably with the results of other researchers and with the results of model experiments.

The use of the family of elements is particularly advantageous during the preliminary design stage of bridge decks or in situations where a full three-dimensional finite element is unnecessary.

References

1. Barsoum, R. S., R. H. Gallagher. Finite Element Analysis of Torsional-Flexural Stability Problems.— Int. J. Numer. Meth. Eng., Vol. 2, 1970, pp. 335-352.
2. Bazant, Z., M. El Nimeiri. Stiffness Method for Curved Box Girders at Initial Stress. — Journal of the Structural Division, ASCE, Vol. 100 No ST10, Proc. Paper 10877, Oct. 1974, pp. 2071-2089.
3. Chai Hong Yoo. Bimoment Contribution to Stability of Thin-Walled Assemblages.—Computers and Structures. Vol. 11, No 5, 1980.
4. Ettouney, M. M., J. B. Kirby. Warping Restraint in Three-Dimensional Frames.—Journal of the Structural Division, ASCE, Vol. 107, No ST8, Proc. Paper 16475, Aug. 1981, pp. 1643-1656
5. Hinton, E., A. Razzaque, O. C. Zienkiewicz, J. D. Davies. A Simple Finite Element Solution for Plates of Homogeneons, Sandwich and Cellular Construction. Proc. Inst. Civ. Eng., London, Part 2, 59, March 1975, pp. 43-65.
6. Krahula, J. L. Analysis of Bent and Twisted Bars Using the Finite Element Method.—AIAA Journal, Vol. 5, No 6, June 1967, pp. 1194-1197.
7. Krajcinovic, D. A Consistent Discrete Elements Technique for Thin-Walled Assemblages.—Int. J. of Solids and Structures, 1969, pp. 639-662.
8. Lie, K. H. Analysis of Stress, Stability and Vibration of Truss Bridges (in English). Scientia Sinica, China, Vol XXI, No 6, 1978.
9. Lie, K. H. The Torsional Theory of Truss Girders-Analysis of Torsion, Stability and Vibration of Truss Bridges (in Chinese). People's Communications Press, Beijing, China, 1975.
10. LUSAS — Finite Element Stress Analysis System. User's Manual, Finite Element Analysis Ltd., London, 1980.

11. Mikkola, M. J., J. Paavola. Finite Element Analysis of Box Girders.—Journal of the Structural Division, ASCE, Vol. 106, No ST6, Proc. Paper 15498, June 1980, pp. 1343-1357.
12. Moffatt, K. R., P. J. Dowling. Shear Lag in Steel Box Girder Bridges. The Structural Engineer, Vol. 53, London, Oct. 1975, pp. 439-448.
13. Richmond, B. The Relationship of Box Beam Theories in Bridge Design. Developments in Bridge Design and Construction, Crosby Lockwood and Son Ltd., 1971, pp. 237-245.
14. Vlasov, V. Z. Thin-Walled Elastic Beams (2nd Edition) Israel Program for Scientific Translation Ltd. Jerusalem, 1961.
15. Zhang, S. H. The Finite Element Analysis of Thin-Walled Box Spine-Beam Bridges. Ph. D. Thesis, The City University, London, Feb. 1982.
16. Zienkiewicz, O. C., J. M. Too. Reduced Integration Technique in General Analysis of Plates and Shells. — Int. J. Numer. Meth. Eng., Vol. 3, 1971.
17. Zyl, S. F. V. Analysis of Curve Segmentally Erected Prestressed Concrete Box Girder Bridges. Ph. D. Thesis, University of California, Berkeley, June 1978.

Received 3. 02. 1987